mdx muscle pathology is independent of nNOS perturbation

Rachelle H. Crosbie[1], Volker Straub[1], Hye-Young Yun[2], Jane C. Lee[1], Jill A. Rafael[3,+], Jeffrey S. Chamberlain[3], Valina L. Dawson[2], Ted M. Dawson[2] and Kevin P. Campbell[1,*]

[1]Howard Hughes Medical Institute, Department of Physiology and Biophysics, Department of Neurology, University of Iowa College of Medicine, Iowa City, IA 52242, USA, [2]Departments of Neurology and Neuroscience, Johns Hopkins University School of Medicine, 600 North Wolfe Street, Baltimore, MD 21287, USA and [3]Department of Human Genetics, University of Michigan, Ann Arbor, MI 48109, USA

In skeletal muscle, neuronal nitric oxide synthase (nNOS) is anchored to the sarcolemma via the dystrophin–glycoprotein complex. When dystrophin is absent, as in Duchenne muscular dystrophy patients and in *mdx* mice, nNOS is mislocalized to the interior of the muscle fiber where it continues to produce nitric oxide. This has led to the hypothesis that free radical toxicity from mislocalized nNOS may contribute to *mdx* muscle pathology. To test this hypothesis directly, we generated mice devoid of both nNOS and dystrophin. Overall, the nNOS–dystrophin null mice maintained the dystrophic characteristics of *mdx* mice. We evaluated the mice for several features of the dystrophic phenotype, including membrane damage and muscle morphology. Removal of nNOS did not alter the extent of sarcolemma damage, which is a hallmark of the dystrophic phenotype. Furthermore, muscle from nNOS–dystrophin null mice maintain the histological features of *mdx* pathology. Our results demonstrate that relocalization of nNOS to the cytosol does not contribute significantly to *mdx* pathogenesis.

INTRODUCTION

Muscular dystrophy represents a group of skeletal muscle diseases that are characterized primarily by progressive muscle wasting and weakness. In the case of Duchenne muscular dystrophy (DMD) and the murine model (*mdx* mouse) for this disease, mutations in the dystrophin gene result in the absence of dystrophin and loss of the dystrophin–glycoprotein complex (DGC) (1–4). This oligomeric complex spans the sarcolemma and links the intracellular actin cytoskeleton to the extracellular matrix (5). Exactly how absence of the DGC leads to muscle cell necrosis is not clearly understood, but several lines of evidence

suggest that oxidative stress may play an important role (6). The possibility that an imbalance of free radicals contributes to the necrotic process in muscular dystrophy was proposed in 1971 by Mendell *et al.* (7), who noted the similarity between oxidative lesions of ischemic muscle and some of the pathologic features of muscular dystrophy. The free radical damage hypothesis was strengthened by experiments which showed elevated levels of free radical-scavenging enzymes in dystrophic muscle, suggesting that expression of these proteins was induced as a result of oxidative stress (8).

Recently, several laboratories have shown that the free radical-producing enzyme neuronal nitric oxide synthase (nNOS; type I) is anchored to the sarcolemma by the DGC (9,10). The PDZ domain of nNOS interacts directly with syntrophin, which is associated with dystrophin (10). In the absence of dystrophin, nNOS is mislocalized to the cytosol where it maintains some of its enzymatic activity (9,11), namely conversion of arginine to citrulline and nitric oxide. Nitric oxide is a highly reactive molecule that potentially can modify lipids, proteins and DNA through a variety of mechanisms (12–16). These observations have led to the hypothesis that free radicals from mislocalized nNOS may contribute to *mdx* muscle pathology (6,9). Regulation of nNOS activity, which normally occurs via Ca^{2+}-calmodulin (17–19), may be altered by elevated levels of intracellular Ca^{2+} present in *mdx* muscle (17–19). The possible aberrant activation of nNOS activity might also contribute to inappropriate free radical production.

Using mice expressing various dystrophin transgenes, we found a correlation between the *mdx* phenotype and the absence of nNOS from the sarcolemma, supporting the hypothesis that mislocalization of nNOS may contribute to the dystrophic phenotype. To test this hypothesis directly, we genetically removed nNOS from *mdx* mice and examined the phenotype of these nNOS–dystrophin null mice. We found that the nNOS–dystrophin double knockout mice maintained the dystrophic phenotype, suggesting that relocalization of nNOS to the cytosol does not significantly contribute to *mdx* pathogenesis.

*To whom correspondence should be addressed. Tel: +1 319 335 7867; Fax: +1 319 335 6957; Email: kevin-campbell@uiowa.edu
+Present address: Genetics Laboratory, Department of Biochemistry, University of Oxford, South Parks Road, Oxford OX1 3QU, UK

Table 1. Effects of dystrophin transgenes on nNOS and DGC sarcolemma localization and muscle morphology

Dystrophin[a]	Deleted region in transgene	Muscle morphology	nNOS	DGC[b]
Wild-type	no deletion	normal	+	+
mdx	premature stop	dystrophic	–	–
Δ3–7 (Δabd)[c]	actin-binding domain	quasi-normal (specific force of muscle intermediate between wt and *mdx*)	+/–	+
Δ17–48 (becker)[d]	rod domain	quasi-normal (slightly elevated central nucleation)	+	+
Δ1–62 (Dp71)[e]	N-terminus and rod domain	dystrophic	–	+
Δ64–67[f]	Cys-rich domain	dystrophic	–	–
Δ68–70[f]	C-terminus	dystrophic	–	–
Δ71–74 (Δ330)[f,g]	syntrophin-binding domain	normal	+	+
Δ75–78[f]	C-terminus	normal	+	+

[a]The dystrophin transgenes are referred to by the deleted exons (i.e. Δ64–67 is missing exons 64–67), with other names given in parentheses.
[b]Dystrophin–glycoprotein complex.
[c]Corrado *et al.*, 1996; [d]Phelps *et al.*, 1995; [e]Cox *et al.*, 1994; Greenberg *et al.*, 1994; [f]Rafael *et al.*, 1996; [g]Rafael *et al.*, 1994.

RESULTS AND DISCUSSION

Absence of nNOS correlates with *mdx* phenotype

In order first to explore the role of nNOS in *mdx* pathology, we examined nNOS expression in a collection of seven dystrophin transgenic mice. The transgenes, which individually were expressed on an *mdx* background, encode truncated dystrophin products (20–26). Muscle from the transgenic mice was evaluated previously for its morphology and for the ability of the transgene to restore sarcolemma localization of the DGC (Table 1).

We detected nNOS expression in skeletal muscle cross-sections by immunofluorescence staining with nNOS antibodies for each of the transgenic mice. These results, summarized in Table 1, suggest a correlation between the *mdx* phenotype and the absence of nNOS from the sarcolemma. We found sarcolemma staining of nNOS in muscle from the Δ3–7 (26) (deletion of the actin-binding domain), Δ17–48 (24) (becker), Δ71–74 (23,25) (formerly referred to as the Δ330) and Δ75–78 (25) mice, which have normal or quasi-normal muscle morphology (Fig. 1). However, nNOS staining was not detected in muscle from the Δ1–62 (21) (Dp71), Δ64–67 (25) and Δ68–70 (25) mice, which maintain the dystrophic, *mdx* phenotype. Interestingly, expression of the Dp71 transgene restores the DGC complex to the sarcolemma, but is not able to rescue the *mdx* morphology (21,22). Chao *et al.* found similar results with the Dp71 mouse (27); however, our results differ concerning the Δ17–48 mouse. The differences observed between the two studies are likely to be due to mouse to mouse variations in the level of Δ17–48 transgene expression, which has been shown to affect the ability of this specific transgene to rescue the *mdx* phenotype (24). Taken together, these data support the hypothesis put forward by Bredt *et al.* (9) that free radicals produced from mislocalized nNOS may contribute to the pathogenesis of muscular dystrophy.

Genetic removal of nNOS from *mdx* mice

To test directly whether misregulated or mislocalized nNOS activity contributes to the pathogenesis of muscular dystrophy, we genetically removed nNOS from *mdx* mice. This was accomplished by mating nNOS^{−/−} males (28) with *mdx* females, as depicted in Figure 2a. The *mdx* phenotype is inherited as an X-linked recessive trait, which stems from a premature stop codon in the dystrophin gene, leading to complete absence of dystrophin (29–31). The nNOS^{−/−} mice were created by a targeted removal of exon 1, which deletes the first 200 amino acids of the protein encoding the PDZ domain. Muscle from nNOS mutant mice specifically lacks the alpha and mu isoforms of nNOS (nNOSα and nNOSμ), which are the only isoforms that bind to the DGC (10). Beta and gamma isoforms of nNOS (nNOSβ and nNOSγ) are not affected by the targeted disruption of this gene (10). However, nNOSβ is not expressed in muscle, and nNOSγ, which has nearly negligible activity (3% catalytic activity compared with nNOSα and nNOSμ), is cytosolic and does not bind to the DGC (10).

In our study, the dystrophin–nNOS mutant (*mdx*:nNOS^{−/−}) mice were identified by PCR genotyping (Fig. 2b) and Southern analysis (data not shown). These data were confirmed by northern analysis showing that nNOS transcript was present in *mdx* mice, but completely absent from nNOS^{−/−} mutant and *mdx*:nNOS^{−/−} mutant mice (Fig. 2c). Western blot analysis of total muscle homogenates and skeletal muscle membranes confirmed that nNOS is mislocalized in *mdx* mice, as previously shown (9,10), and that the nNOS^{−/−} and *mdx*:nNOS^{−/−} mice lacked nNOS at the protein level (data not shown).

We have tested the *mdx*:nNOS^{−/−} mice for several characteristics of the *mdx* phenotype and, overall, we found that the *mdx*:nNOS^{−/−} mice maintained these *mdx* features. The *mdx*:nNOS^{−/−} mice were examined up to 12 months of age, and we found no quantitative differences compared with *mdx* mice, suggesting that the disease pathogenesis was not altered by nNOS removal.

mdx:nNOS^{−/−} mice maintain membrane damage

Sarcolemma damage is one of the early hallmarks of *mdx* pathology (32–34). The possibility that free radicals from mislocalized nNOS contribute to sarcolemma damage is consistent with the observations of Rando (35), Ragusa (36) and their colleagues, who recently reported elevated levels of lipid peroxidation in muscles of *mdx* mice. This disruption in membrane integrity permits unregulated exchange of molecules between the circulating blood serum and the muscle fiber. We evaluated membrane damage in the nNOS–dystrophin mutant mice by employing two different assays. First, permeability of the
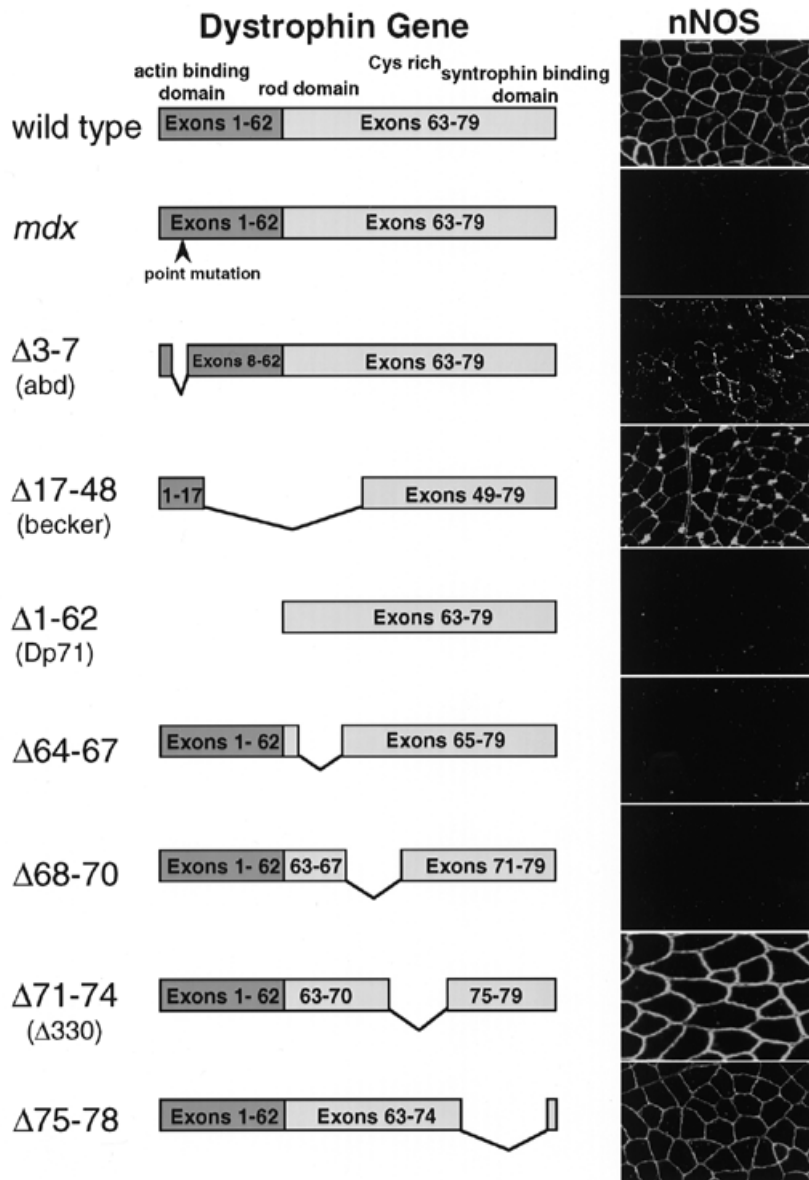
Figure 1. Immunohistochemical analysis of nNOS in muscle from dystrophin transgenic mice. Skeletal muscle cryosections from wild-type, *mdx*, Δ3–7 (deletion of the actin-binding domain), Δ17–48 ('becker'), Δ1–62 (Dp71), Δ64–67, Δ68–70, Δ71–74 (formerly referred to as Δ330) and Δ75–78 mice were stained with an affinity-purified rabbit polyclonal antibody against the N-terminal domain of nNOS. The dystrophin transgenes are depicted schematically on the right of each panel. Skeletal muscle which maintains the *mdx* morphology does not have sarcolemma staining of nNOS. Bar indicates 100 μm.

muscle fiber was analyzed by evaluating leakage of muscle-specific pyruvate kinase (PK) in the blood serum (Fig. 3a). Wild-type and nNOS mutant mice have low serum levels of PK activity. *mdx* mice, on the other hand, exhibit high serum levels of PK activity. The PK activities in the serum of *mdx*:nNOS$^{-/-}$ mice were similar to that of *mdx* mice, indicating that membrane damage persisted despite the removal of nNOS.

To examine leakage into the muscle fiber, we employed an Evans blue tracer assay (37,38). This intravenously injected fluorescent dye accumulates in the interior of damaged muscle fibers presumably by entering through unrepaired tears in the membrane. Work from several groups has demonstrated that skeletal muscle fibers from *mdx* mice exhibit intracellular Evans blue staining (37,38). With the Evans blue injections, we demonstrated that extensive membrane damage was present in quadriceps muscle from both *mdx* and *mdx*:nNOS$^{-/-}$ mutant mice (Fig. 3b). We have also examined the diaphragm muscle from these mice and found that Evans blue accumulated to the same extent in *mdx* and *mdx*:nNOS$^{-/-}$ mice. These data are consistent with the pyruvate kinase measurements.

mdx:nNOS$^{-/-}$ muscle maintains dystrophic morphology

Additional features of *mdx* muscle pathology include necrosis, variation in fiber size and increased fiber degeneration/regeneration with centrally located nuclei. Hematoxylin and eosin (H&E) staining of quadriceps muscle cross-sections clearly showed the presence of these pathological features in age-
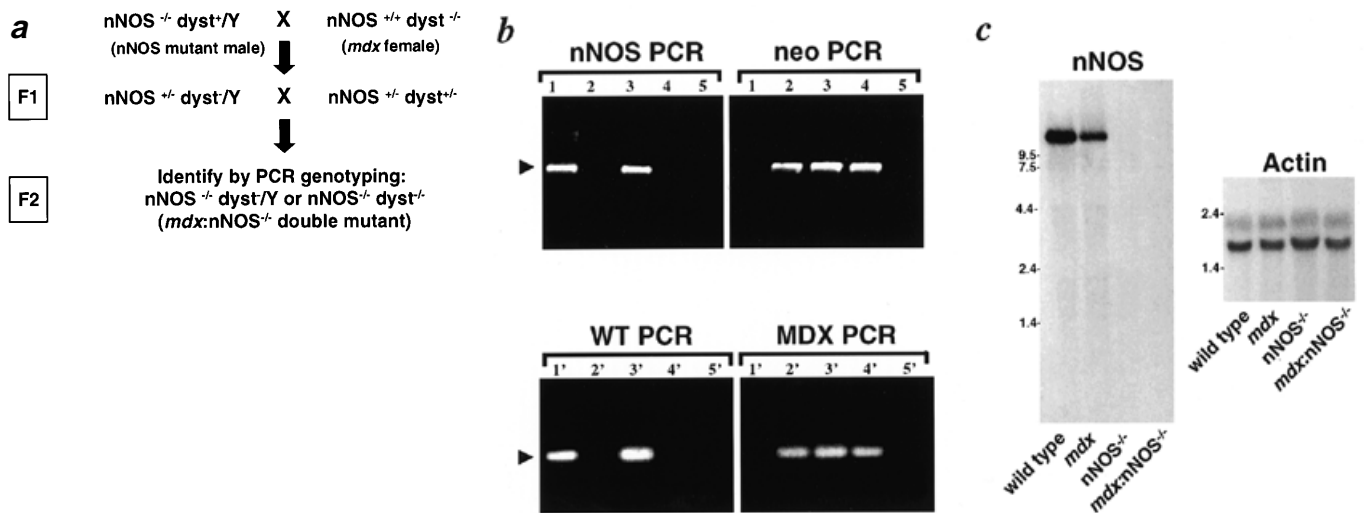
Figure 2. Generation of dystrophin–nNOS double mutant mice. (**a**) Breeding scheme to produce *mdx* mice devoid of nNOS. nNOS single mutant males (nNOS$^{-/-}$ dyst$^+$/Y) were bred with *mdx* females (nNOS$^{+/+}$ dyst$^{-/-}$) to produce heterozygote F1 offspring. F1 generation mice were intercrossed to produce F2 generation mice with a one in eight prospect for obtaining mice with an nNOS and dystrophin double mutant genotype (nNOS$^{-/-}$ dyst$^{-/-}$, female or nNOS$^{-/-}$ dyst$^-$/Y, male). (**b**) nNOS–dystrophin genotyping by PCR amplifications. Upper panel: for nNOS genotyping, separate amplifications were performed using *neo*-specific (neo PCR) or *nNOS*-specific (nNOS PCR) primers. The *neo* gene was used in the targeted disruption of the *nNOS* gene (28) and therefore serves as a marker for the nNOS mutant allele. PCR amplifications were performed using genomic DNA from wild-type (lane 1), nNOS mutant (lane 2), nNOS heterozygous (lane 3) and *mdx*:nNOS$^{-/-}$ mutant (lane 4) mice. Lane 5 is a no-DNA template control. The arrowhead marks the 500 bp product that is expected for both the neo and nNOS PCR reactions. Heterozygous females (nNOS$^{-/-}$ dyst$^{-/-}$) can be distinguished by this PCR-based method. Note the presence of PCR products for both *neo* and *nNOS* in lanes 3 as well as PCR products for *mdx* and wild-type dystrophin alleles in lanes 3′. Lower panel: offspring were genotyped for the *mdx* allele using PCR analysis based on the *mdx* amplification-resistant mutation system (*mdx*-ARMS) (41). For each DNA sample, two sets of PCRs are utilized. One PCR set utilizes a reverse oligonucleotide primer specific for the wild-type allele (WT PCR) and therefore only allows amplification of the wild-type allele. The second PCR reaction utilizes a reverse oligonucleotide primer specific for the *mdx* allele (MDX PCR) and therefore only amplifies the *mdx* allele. The same forward primer is used in each reaction. The PCR product for each amplification is 105 bp. Genotyping was performed for wild-type (lane 1′), *mdx* (lane 2′), *mdx* heterozygous (lane 3′) and *mdx*:nNOS$^{-/-}$ (lane 4′) genomic DNA. Lane 5′ is a no DNA template control. (**c**) Analysis of nNOS expression in mouse skeletal muscle. Northern blots of total RNA (20 μg/lane) from wild-type, *mdx*, nNOS$^{-/-}$ and *mdx*:nNOS$^{-/-}$ skeletal muscle were hybridized with ^{32}P-labeled nNOS probe (left panel). As a control for loading, the same blot was probed with β-actin (right panel). Molecular size standards (in kilobases) are indicated on the left of each panel.

matched *mdx*:nNOS$^{-/-}$ mice, indicating that these characteristics of the *mdx* phenotype were independent of nNOS (Fig. 4a). H&E staining of the diaphragm muscle showed that the *mdx*:nNOS$^{-/-}$ mice maintained the hallmark features of the *mdx* morphology (data not shown). Quantitation of central nucleation for both muscle types demonstrated that the *mdx*:nNOS$^{-/-}$ mice had undergone levels of regeneration identical to the *mdx* mice (Fig. 4b). We have examined the *mdx*:nNOS$^{-/-}$ mice up to 12 months of age and found no quantitative differences compared with *mdx* mice, suggesting that the disease pathogenesis is not altered by nNOS removal.

nNOS is anchored to the sarcolemma by its association with the DGC. In addition to dystrophin, the DGC is composed of the sarcoglycans, syntrophins and dystroglycan (1–5). Sarcospan (25 kDa) is the most recently identified member of the DGC, and is unique in that it is predicted to have four transmembrane-spanning domains (43). Although nNOS is not an integral component of this complex, it is linked to dystrophin via attachment to the PDZ domain of sytrophin (9,10). Interestingly, syntrophin has been shown to bind to the voltage-gated sodium channels in skeletal and cardiac muscle, suggesting that nNOS may regulate these channels *in vivo* (44).

Our results suggest that redirection of nNOS from the sarcolemma to the cytoplasm in *mdx* muscle is not likely to be critical for the oxidative damage and other necrotic processes observed in muscular dystrophy. Although we cannot rule out that

cytosolic nNOS may contribute partially to these events, its contribution must be minimal, given the extent of damage observed in the *mdx*:nNOS$^{-/-}$ mice. Furthermore, knowledge of the prerequisite factors necessary for restoring normal muscle morphology is imperative for designing strategies to alleviate the dystrophic phenotype.

Our results support the idea that removing cytosolic nNOS from *mdx* muscle is not essential for correcting the *mdx* phenotype. It is possible, though, that loss of nNOS function at the sarcolemma contributes to the muscular dystrophy pathogenesis. For instance, several reports have documented that nitric oxide produced by nNOS can provide protection from more toxic free radicals (16). Perhaps loss of this protective function is the basis for elevated oxidative stress in dystrophic muscle. Defining the functional interactions between nNOS and the DGC will provide insight into the role of nNOS at the sarcolemma.

MATERIALS AND METHODS

Mice

Wild-type (C57BL/10) and *mdx* (C57BL/10ScSn) mice, obtained from Jackson Laboratories, were maintained at the University of Iowa Animal Care Unit in accordance with animal usage guidelines. *mdx* mice were maintained as a breeder colony of *mdx* males and homozygous *mdx* females. nNOS single mutant mice
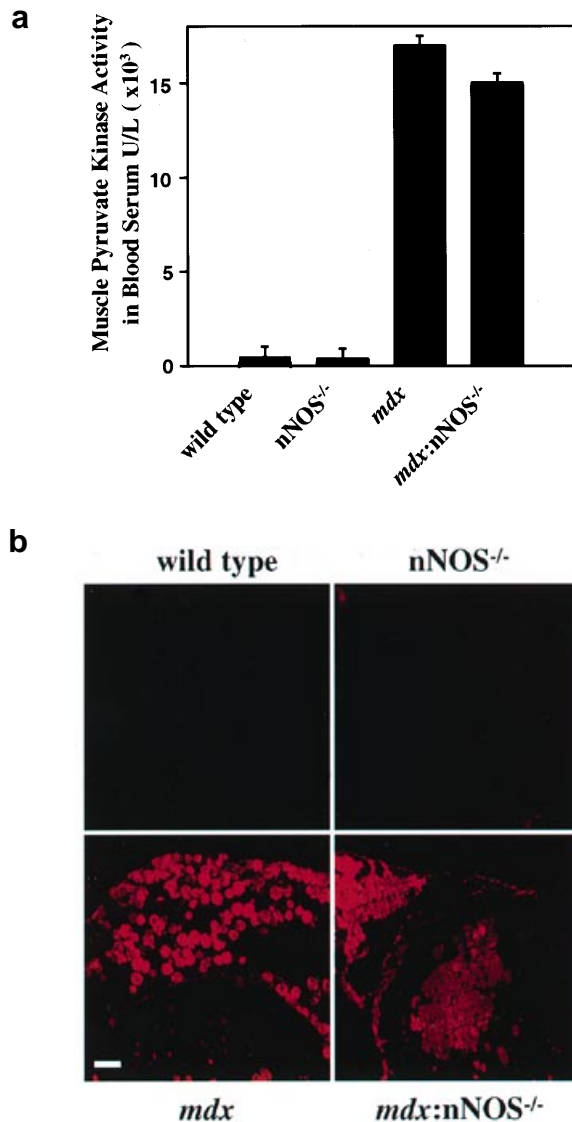
a

b

Figure 3

b

wild type   nNOS⁻ᐟ⁻

mdx   *mdx*:nNOS⁻ᐟ⁻

Figure 3. Serum pyruvate kinase and Evans blue assays detect sarcolemma damage. (**a**) Measurement of pyruvate kinase released from the muscle fiber into the circulating blood. Pyruvate kinase activities were evaluated in the blood serum from wild-type, *mdx*, nNOS⁻ᐟ⁻ and *mdx*:nNOS⁻ᐟ⁻ mice. Error bars indicate the deviation between six sets of experiments (duplicate measurements for three separate mice). (**b**) Evans blue assay for infiltration of blood serum proteins into the muscle fiber. Intravenous injection of the Evans blue tracer can be detected in fibers with damaged plasma membranes. Transverse cross-sections of quadriceps muscle were observed with a fluorescence confocal microscope equipped with green activation filters. Evans blue-positive fibers are denoted by red staining. Bar, 100 µm.

(C57BL/6) were obtained from the colony produced by Huang *et al.* (28). The targeted disruption of the *nNOS* gene in these mice was accomplished previously by replacement of exon 1 with the neomycin resistance gene (*neo*) through homologous recombination (28). The dystrophin transgenic mice have been described previously (21,24–26,39)
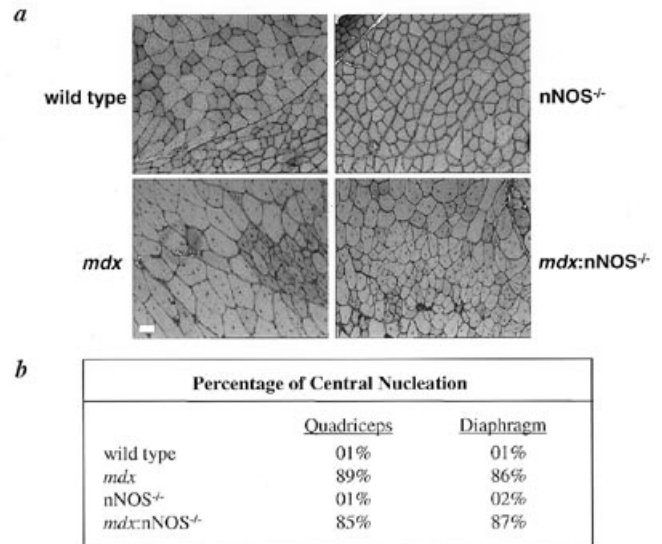

a

wild type   nNOS⁻ᐟ⁻

mdx   *mdx*:nNOS⁻ᐟ⁻

b

Percentage of Central Nucleation		
	Quadriceps	Diaphragm
wild type	01%	01%
mdx	89%	86%
nNOS⁻ᐟ⁻	01%	02%
mdx:nNOS⁻ᐟ⁻	85%	87%

Figure 4. Skeletal muscle morphology of wild-type, *mdx*, nNOS⁻ᐟ⁻ and *mdx*:nNOS⁻ᐟ⁻ mice. (**a**) H&E staining of quadriceps sections shows that the *mdx*:nNOS⁻ᐟ⁻ mutant mice maintain the characteristics of *mdx* pathology, including variations in fiber size, centrally located nuclei and phagocytic infiltration. Identical morphological features were found in diaphragm muscle (not shown). (**b**) Quantitation of central nucleation for both quadriceps and diaphragm muscles. Central nucleation is represented as the percentage of total nucleated fibers with centrally located nuclei.

Antibodies

Anti-nNOS antibodies were generated by intramuscular and subcutaneous injection of New Zealand white rabbits (Knapp Creek Farms) with 500 µg of an nNOS (rat amino acids 1–200)–glutathione *S*-transferase (GST) fusion protein in an emulsion of Freund's complete adjuvant (Sigma). Rabbits 200 and 201 were boosted 2 weeks later with an s.c. injection of nNOS–GST fusion protein (1 mg) in TBS (20 mM Tris–HCl, 100 mM NaCl, pH 7.5). Blood serum was collected from the rabbits 1 week following the boost and tested for the presence of anti-nNOS antibodies. The serum was cleared of anti-GST antibodies with Immobilon-P (Millipore) strips containing GST and subsequently affinity-purified using nNOS–GST Immobilon-P strips. C-terminal dystrophin antibodies were affinity-purified from goat 20 (immunized with the DGC complex) (40) using dystrophin (mouse C-terminal 315 amino acids)–GST Immobilon-P strips.

Immunofluorescence

Transverse cryosections (7 µm thick) from mouse quadriceps were fixed with 4% freshly depolymerized paraformaldehyde for 10 min at room temperature. Muscle sections were washed briefly with TBS and incubated with affinity-purified nNOS antibodies (1:10 dilution; rabbit 200) for 24 h.

Generation and genotyping of dystrophin–nNOS double mutant mice

nNOS single mutant males were bred with *mdx* females in the breeding strategy outlined in Figure 2a. Heterozygous F1

offspring were mated to produce F2 generation mice. Identification of the dystrophin–nNOS mutant mice was performed by PCR genotyping of genomic DNA prepared from mouse tail snips (41). DNA from wild-type, *mdx* and nNOS single mutant mice were used for controls.

mdx genotyping. An amplification-resistant mutation system (ARMS) assay was used to screen for the *mdx* point mutation as previously described (41). Briefly, two separate PCR reactions were performed. One reaction (MDX PCR) utilizes oligonucleotide primers which only allow amplification of the *mdx* allele, and the second PCR reaction (WT PCR) amplifies only the wild-type allele (41). Both PCR products are 105 bp.

nNOS genotyping. PCR amplification of *nNOS* exon 1 (which is disrupted in the nNOS mutant mice) was performed with mouse tail DNA using either *nNOS*- or *neo*-specific oligonucleotides. PCR primers for the *neo* and *nNOS* amplifications were as follows: 5′-TGGAGAGGCTATTCGGCTATGAC-3′ (*neo*, sense); 5′-CACCATGATATTCGGCAAGCAC-3′ (*neo*, antisense); 5′-ATCTCAGATCTGATCCGAGGAG-3′ (*nNOS*, sense); 5′-CTTTCATCTCTGCTTTGGCTGG-3′ (*nNOS*, antisense). PCR cycling conditions were 94°C, 45 s; 55°C, 45 s; 72°C, 45 s for 35 cycles in a buffer consisting of 10 mM Tris–HCl, 1.5 mM $MgCl_2$, 50 mM KCl, pH 8.3. The PCR product for both reactions was 500 bp. The genotyping was confirmed by Southern analysis (28) (data not shown).

Northern blot analysis

Total RNA from skeletal muscle of wild-type, *mdx*, nNOS$^{-/-}$ and *mdx*:nNOS$^{-/-}$ mice was isolated using RNAzol (Tel-Test, Friendswood, TX) according to the manufacturer's directions. The RNA (20 μg/lane) was fractionated by electrophoresis through a 1.25% agarose, 5% formaldehyde gel and overnight transfer to Biosbrane membranes by capillary action. Northern blot filters were hybridized with a radiolabeled cDNA probe encoding the first N-terminal 200 residues of rat nNOS. Hybridization was carried out using standard methods, and blots were exposed for autoradiography.

Pyruvate kinase assay

The activities of muscle-specific PK isozyme found in the blood serum were measured as previously documented (42). Blood was collected from the retroorbital sinus of 4- to 12-week-old mice and the serum was stored at –80°C prior to measurements. Data shown in all figures are from 8-week-old mice.

Evans blue assay

Evans blue dye (10 mg/ml) dissolved in phosphate-buffered saline (10 mM phosphate buffer, 150 mM NaCl, pH 7.4) was sterile filtered using a 0.2 μm pore filter. The Evans blue was injected into the tail vein of the mouse (0.1 ml/10 g body weight). The mice were euthanized 5–8 h after injection. Quadriceps muscle was prepared and observed under a Bio-Rad MRC-600 laser scanning confocal microscope as described previously (37,38). Digitized images were captured under identical conditions.

Histology

Transverse cross-sections (10 μm) of quadriceps and diaphragm were fixed for 10 min at room temperature with 10% freshly depolymerized paraformaldehyde. Muscle sections were washed briefly with TBS and stained with H&E. Sections were visualized with a Leitz diaplan light microscope, and digitized images were captured under identical conditions. To quantitate central nucleation, histological sections were photographed, and the percentage of centrally nucleated myofibers was determined by dividing the number of myofibers containing one or more centrally located nuclei by the total number of nucleated fibers. Myofibers with no nuclei in the plane were not counted. On average, 1200 myofibers were counted for both quadriceps and diaphragm.

REFERENCES

1. Ohlendieck, K. and Campbell, K.P. (1991) Dystrophin-associated proteins are greatly reduced in skeletal muscle from *mdx* mice. *J. Cell Biol.*, **115**, 1685–1694.
2. Ohlendieck, K. (1993) Duchenne muscular dystrophy: deficiency of dystrophin-associated proteins in the sarcolemma. *Neurology*, **43**, 795–800.
3. Ibraghimov-Beskrovnaya, O., Ervasti, J.M., Leveille, C.J, Slaughter, C.A., Sernett, S.W. and Campbell, K.P. (1992) Primary structure of dystrophin-associated glycoproteins linking dystrophin to the extracellular matrix. *Nature*, **355**, 696–702.
4. Ervasti, J.M., Ohlendieck, K., Kahl, S.D., Gaver, M.G. and Campbell, K.P. (1990) Deficiency of a glycoprotein component of the dystrophin complex in dystrophic muscle. *Nature*, **345**, 315–319.
5. Campbell, K.P. (1995) Three muscular dystrophies: loss of cytoskeleton–extracellular matrix linkage. *Cell*, **80**, 675–679.
6. Brown, R.H. (1995) Free radicals, programmed cell death and muscular dystrophy. *Curr. Opin. Neurol.*, **8**, 373–378.
7. Mendell, J.R., Engel, W.K. and Derrer, E.C. (1971) Duchenne muscular dystrophy: functional ischemia reproduces its characteristic lesions. *Science*, **172**, 1143–1145.
8. Mizuno, Y. (1984) Changes in superoxide dismutase, catalase, glutathione peroxidase, and glutathione reductase activities and thiobarbituric acid-reactive products levels in early stages of development in dystrophic chickens. *Exp. Neurol.*, **84**, 58–73.
9. Brenman, J.E., Chao, D.S., Xia, H., Aldape, K. and Bredt, D.S. (1995) Nitric oxide synthase complexed with dystrophin and absent from skeletal muscle sarcolemma in Duchenne muscular dystrophy. *Cell*, **82**, 743–752.
10. Brenman, J.E., Chao, D.S., Gee, S.H., McGee, A.W., Craven, S.E., Santillano, D.R., Wu, Z., Huang, F., Xia, H., Peters, M.F., Froehner, S.C. and Bredt, D.S. (1996) Interaction of nitric oxide synthase with the postsynaptic density protein PSD-95 and alpha-1-syntrophin mediated by PDZ domains. *Cell*, **84**, 757–767.
11. Chang, W.J., Iannaccone, S.T., Lau, K.S., Masters, B.S.S., McCabe, T.J., McMillan, K., Padre, R.C., Spencer, M.J., Tidball, J.G. and Stull, J.T. (1996) Neuronal nitric oxide synthase and dystrophin-deficient muscular dystrophy. *Proc. Natl Acad. Sci. USA*, **93**, 9142–9147.
12. Yun, H.-Y., Dawson, V.L. and Dawson, T.M. (1996) Neurobiology of nitric oxide. *Crit. Rev. Neurobiol.*, **10**, 291–316.
13. Moncada, S. and Higgs, A. (1993) The L-arginine–nitric oxide pathway. *New Engl. J. Med.*, **329**, 2002–2012.

14. Nathan, C. and Xie, Q.W. (1994) Nitric oxide synthases: roles, tolls, and controls. *Cell*, **78**, 915–918.

15. Marletta, M.A. (1994) Nitric oxide synthase: aspects concerning structure and catalysis. *Cell*, **78**, 927.

16. Beckman, J.S. (1991) The double-edged role of nitric oxide in brain function and superoxide-mediated injury. *J. Dev. Physiol.*, **15**, 53–59.

17. Bertorini, T.E., Bhattacharya, S.K., Palmieri, G.M, Chesney, C.M., Pifer, D. and Baker, B. (1982) Muscle calcium and magnesium content in Duchenne muscular dystrophy. *Neurology*, **32**, 1088–1092.

18. Jackson, M.J., Jones, D.A. and Edwards, R.H. (1985) Measurements of calcium and other elements in muscle biopsy samples from patients with Duchenne muscular dystrophy. *Clin. Chim. Acta*, **147**, 215–221.

19. Turner, P.R., Fong, P.Y., Denetclaw, W.F. and Steinhardt, R.A. (1991) Increased calcium influx in dystrophic muscle. *J. Cell Biol.*, **115**, 1701–1712.

20. Corrado, K., Mills, P.L. and Chamberlain, J.S. (1994) Deletion analysis of the dystrophin–actin binding domain. *FEBS Lett.*, **344**, 255–260.

21. Cox, G.A., Sunada, Y., Campbell, K.P. and Chamberlain, J.S. (1994) Dp71 can restore the dystrophin-associated glycoprotein complex in muscle but fails to prevent dystrophy. *Nature Genet.*, **8**, 333–339.

22. Greenberg, D.S., Sunada, Y., Campbell, K.P., Yaffe, D. and Nudel, U. (1994) Exogenous Dp71 restores the levels of dystrophin associated proteins but does not alleviate muscle damage in *mdx* mice. *Nature Genet.*, **8**, 340–344.

23. Rafael, J.A., Sunada, Y., Cole, N.M, Campbell, K.P., Faulkner, J.A. and Chamberlain, J.S. (1994) Prevention of dystrophic pathology in *mdx* mice by a truncated dystrophin isoform. *Hum. Mol. Genet.*, **3**, 1725–1733.

24. Phelps, S.F., Hauser, M.A., Cole, N.M., Rafael, J.A., Hinkle, R.T., Faulkner, J.A. and Chamberlain, J.S. (1995) Expression of full-length and truncated dystrophin mini-genes in transgenic *mdx* mice. *Hum. Mol. Genet.*, **4**, 1251–1258.

25. Rafael, J.A., Cox, G.A., Corrado, K., Jung, D., Campbell, K.P. and Chamberlain, J.S. (1996) Forced expression of dystrophin deletion constructs reveals structure–function correlations. *J. Cell Biol.*, **134**, 93–102.

26. Corrado, K., Rafael, J.A., Mills, P.L., Cole, N.M., Faulkner, J.A., Wang, K. and Chamberlain, J.S. (1996) Transgenic *mdx* mice expressing dystrophin with a deletion in the actin-binding domain display a 'mild Becker' phenotype. *J. Cell Biol.*, **134**, 873–884.

27. Chao, D.S., Gorospe, J.R.M., Brenman, J.E., Rafeal, J.A., Peters, M.F., Froehner, S.C., Hoffman, E.P., Chamberlain, J.S. and Bredt, D.S. (1996) Selective loss of sarcolemmal nitric oxide synthase in Becker muscular dystrophy. *J. Exp. Med.*, **184**, 609–618.

28. Huang, P.L., Dawson, T.M., Bredt, D.S., Snyder, S.H. and Fishman, M.C. (1993) Targeted disruption of the neuronal nitric oxide synthase gene. *Cell*, **75**, 1273–1286.

29. Bulfield, G., Siller, W.G., Wright, P.A. and Moore, K.J. (1984) X chromosome-linked muscular dystrophy (*mdx*) in the mouse. *Proc. Natl Acad. Sci. USA*, **81**, 1189–1192.

30. Hoffman, E.P., Brown, R.H. and Kunkel, L.M. (1987) Dystrophin: the protein product of the Duchenne muscular dystrophy locus. *Cell*, **51**, 919–928.

31. Chamberlain, J.S., Pearlman, J.A., Muzny, D.M., Gibbs, R.A., Ranier, J.E., Caskey, C.T. and Reeves, A.A. (1988) Expression of the murine Duchenne muscular dystrophy gene in muscle and brain. *Science*, **239**, 1416–1418.

32. Weller, B., Karpati, G. and Carpenter, S. (1990) Dystrophin-deficient *mdx* muscle fibers are preferentially vulnerable to necrosis induced by experimental lengthening contractions. *J. Neurol. Sci.*, **100**, 9–13.

33. Menke, A. and Jockusch, H. (1991) Decreased osmotic stability of dystrophin-less muscle cells from the *mdx* mouse. *Nature*, **349**, 69–71.

34. Petrof, B.J., Shrager, J.B., Stedman, H.H., Kelly, A.M. and Sweeney, H.L. (1993) Dystrophin protects the sarcolemma from stresses developed during muscle contraction. *Proc. Natl Acad. Sci. USA*, **90**, 3710–3714.

35. Rando, T.A., Dziesietnik, M.-H., Dhawan, J., Yu, Y. and Whirl, M. (1997) Oxidative injury precedes muscle necrosis in dystrophin-deficient (*mdx*) mice. *Neurology*, **48**, abstract P06.135.

36. Ragusa, R.J., Chow, C.K. and Porter, J.D. (1997) Oxidative stress as a potential pathogenic mechanism in an animal model of Duchenne muscular dystrophy. *Neuromusc. Disord.*, **7**, 379–386.

37. Matsuda, R., Nishikawa, A. and Tanaka, H. (1995) Visualization of dystrophic muscle fibers in *mdx* mouse by vital staining with Evans blue: evidence of apoptosis in dystrophin-deficient muscle. *J. Biochem.*, **118**, 959–964.

38. Straub, V., Rafael, J.A., Chamberlain, J.S. and Campbell, K.P. (1997) Animal models for muscular dystrophy show different patterns of sarcolemmal disruption. *J. Cell Biol.*, **139**, 375–385.

39. Rafael, J.A., Sunada, Y., Cole, N.M., Campbell, K.P., Faulkner, J.A. and Chamberlain, J.S. (1994) Prevention of dystrophic pathology in *mdx* mice by a truncated dystrophin isoform. *Hum. Mol. Genet.*, **3**, 1725–1733.

40. Jung, D., Duclos, F., Apostol, B., Straub, V., Lee, J.C., Allamand, V., Venzke, K.P., Sunada, Y., Moomaw, C.R., Leveille, C.J., Slaughter, C.A., Crawford, T.O., McPherson, J.D. and Campbell K.P. (1996) Characterization of delta-sarcoglycan, a novel component of the oligomeric sarcoglycan complex involved in limb-girdle muscular dystrophy. *J. Biol. Chem.*, **50**, 32321–32329.

41. Amalfitano, A. and Chamberlain, J.S. (1996) The *mdx*-amplification-resistant mutation system assay, a simple and rapid polymerase chain reaction-based detection of the *mdx* allele. *Muscle and Nerve*, **19**, 1549–1553.

42. Edwards, R.J. and Watts, D.C. (1981) Specific spectrophotometric assay for the m isozyme of pyruvate kinase in plasma samples containing mixtures of the muscle (m) and liver (l) isozymes. *Clin. Chem.*, **27**, 906–909.

43. Crosbie, R.H., Heighway, J., Venzke, D.P., Lee, J.C. and Campbell, K.P. (1997) Sarcospan, the 25-kDa transmembrane component of the dystrophin–glycoprotein complex. *J. Biol. Chem.*, **272**, 31221–31224.

44. Gee, S.H., Madhavan, R., Levinson, S.R., Caldwell, J.H., Sealock, R. and Froehner, S.C. (1998) Interaction of muscle and brain sodium channels with multiple members of the syntrophin family of dystrophin-associated proteins. *J. Neurosci.*, **18**, 128–137.